Prediction of fatigue lives at stress raising features in a high strength steel

R.J. Lancaster, M.T. Whittaker, K.M. Perkins, S.P. Jeffs
Materials Research Centre, Swansea University, SA2 8PP

Corresponding Author: Dr. Robert Joseph Lancaster, Materials Research Centre, Swansea University, SA2 8PP, Phone: (01792) 602061, Fax: (01792) 295693, Email: r.j.lancaster@swansea.ac.uk

Abstract

The fatigue properties of the high strength stainless steel CSS42L have been evaluated under strain and stress controlled conditions. The results have been used to derive a predictive approach based on the Walker strain equation. Accurate predictions are obtained for VCN and DEN specimens although the lower stress concentration RCN specimen is shown to compare more readily with plain specimen stress controlled data. The difference in fatigue life between the notched specimens has been found to be related to the crack propagation phase where the crack grows through material which has previously been operating under reduced stress conditions.

Keywords

Steel, Walker Strain, Life Prediction, Fatigue, Notches

1. Introduction

The drive for increased efficiency in the aerospace sector, based on the ACARE 2020 targets, will require contributions across the industry. Evolution of the gas turbine engine through weight reductions and increased operating temperatures will offer a significant contribution as will further developments in airframe structures and air traffic management. The increased power offered by modern gas turbine engines however, has allowed for the production of larger aircraft which offer efficiency savings through increased passenger travel, and hence a lower fuel consumption per passenger kilometre.

The increased weight of modern aircraft means that ever increasing demands are placed on materials used for load bearing parts requiring high strength, good fracture toughness and fatigue resistance, such as landing gear. The typical requirements for these components have led to the use of ultra high strength steels such as 300M although the opportunity for weight saving has led to the employment of high strength beta titanium alloys such as Ti5-3-3 or even potentially organic matrix composites (OMCs) [1]. However, these material systems come at an increased cost, which must be offset against the improvements in density and also corrosion resistance.

The economic case for high strength stainless steels is further improved by the development of new alloys such as CSS42L, which seeks to balance strength with improved corrosion resistance. CSS42L is a case carburizable stainless steel capable of reasonable operation at temperatures over 400°C, although this is of less importance for landing gear applications than other components where the alloy has found employment, typically cams, shafts and bolts.

Of great significance to the employment of these alloys, however, is the provision to accurately life the material under a range of loading conditions and in particular, to characterise the effects of stress raising features which may produce localised plastic deformation which can act as a source for fatigue crack initiation. Previous work [2, 3] has shown that notched specimen fatigue behaviour can most accurately be predicted through use of strain control fatigue results. In principle, material at the notch root will initially be undergoing a higher stress than surrounding material and as such, will

be constrained by this surrounding material which undergoes less deformation. Therefore, under these conditions the material can now be considered to be under a strain controlled rather than stress controlled type of deformation. There is however little information available detailing the degree of constraint necessary to produce these conditions, where a transition to this type of behaviour might occur and furthermore whether it is likely to be material, temperature or environment dependent.

In considering the current work it is necessary to appreciate the previous work which has been conducted in the field so that an appropriate method can be followed if necessary. Glinka [4-6] previously developed an analytical method to calculate the local strains at notches when the deformation is non-linear based on the equivalent strain energy density. The technique assumes the strain energy density in the plastic zone ahead of a notch can be calculated on the basis of the elastic stress-strain solution.

Duran [7] proposed a series of modifications to Glinka's method in order to calculate the inelastic stress-strain fields at notched regions as the stress state becomes biaxial or triaxial. Whereas Glinka's method was designed to estimate stress-strain values at the notch tip after yielding, and therefore low cycle fatigue (LCF) design, Duran's modified technique focuses on the stress fields at the tip of the notch for high cycle fatigue (HCF) considerations. Results showed that the technique offers much promise for monotonic loading and the potential of extending them for fatigue loading under HCF conditions.

Golos and Ellyin [8] also proposed a prediction method for fatigue initiation lives in notched components through a strain energy density approach. This technique has shown promise in predicting notched fatigue behaviour [9] over more traditional strain based methods.

In addition to the more analytical based approaches to determine local notch stresses and strains, numerical methods such as Finite Element (FE), are often employed and have found to be particularly effective in establishing the elastic-plastic stress state during cyclic loading [10, 11].

With reference to the previous literature, the current work seeks to evaluate the results of three notched specimen types designed to be representative of industrial stress raising features. Based on a limited amount of fatigue data an appropriate fatigue lifing method has been proposed from which notched specimen predictions can be made. Conclusions can then be drawn regarding the influence of constraint and the most appropriate method of predicting fatigue life.

2. Experimental method

Commercially available CSS42L was obtained for the research with a chemical composition as detailed in Table 1. A heat treatment procedure was employed in which the material was heated to and maintained at 885^{o}C for 1 hour, then gas quenched down to room temperature. After being cooled to -73^{o}C and held for 1 hour, the material was tempered at 482^{o}C for 5 hours. The microstructure of the material in its tempered form is displayed in Figure 1.

A total of 25 fatigue tests were performed on a servo-hydraulic test machine, 22 under stress controlled conditions and an additional three under strain control, where an MTS 12mm gauge length extensometer was employed to control strain. Testing was conducted at 20°C under controlled laboratory conditions, and an R ratio of 0 was employed whether testing was conducted under stress control (R_{σ}=0) or strain control (R_{ε}=0) and a trapezoidal 1-1-1-1 waveform was applied. The same test specimen was utilised for either stress or strain controlled testing and consisted of a

6mm diameter and 12mm parallel length. Stress or strain was varied from test to test in order to produce a relevant low cycle fatigue curve.

Notched specimen testing was conducted on three different geometries considered to be representative of typical stress raising features in engineering components. These specimens are displayed in Figure 2. The Round-cylindrical notch (RCN) (Figure 2(a)) has a stress concentration factor, K_t of 1.4, the Double-edged notch (DEN) (Figure 2(b)) a K_t of 1.78 and the V-cylindrical notch (VCN) (Figure 2(c)) a K_t of 2.7. Each of these were determined by finite element analysis (FEA). Testing was again conducted at an R ratio of 0 and fatigue curves were generated as previously described. Each notched test piece had potential difference (PD) monitoring attached in an attempt to determine crack initiation during the test through a pulsed direct current.

3. Results

Fatigue tests produced under strain control loading allowed for the recording of stress-strain hysteresis loops, from which plots of applied stress vs. cycles could be derived, required for lifing approaches such as the Walker strain approach. An example of these hysteresis loops is shown in Figure 3, for a peak applied strain of 1% at an R ratio of 0. Full details of the three experiments undertaken in strain control are displayed in table 2. Based on these experiments and further load controlled fatigue tests, Figure 4 illustrates the fatigue response of plain specimens along with that of the three notch types previously described. Strain controlled data is plotted on the y-axis as stabilised stress range, defined as the values calculated at $N_f/2$, where N_f is the strain controlled fatigue life. Load controlled fatigue data is plotted as the nominal stress against fatigue life. Data points designated with an arrow indicate a run out after 1,000,000 cycles.

Clearly evident in the data is the reduction in fatigue life brought about by the introduction of a notch to the specimen. A significant reduction in fatigue life is observed in both the RCN and DEN notch geometries with further reductions in the VCN specimen.

Figure 5 provides further detail of these results by illustrating the potential difference across the notch roots for a selection of the tested notched specimens. Despite the relatively large distance between PD wires it is clear that a clean response is found, allowing for accurate determination of the onset of long crack growth in each case. Initially apparent is the significant difference in crack initiation between the different notch types. Consistently in the VCN specimen a detectable crack forms at approximately 54% of the total fatigue life. However, in both the RCN and DEN specimens cracks are not detected until approximately 73% and 92% respectively. Table 3 provides details about the initiation and propagation lives of specimens for which PD readings were recorded.

4. Discussion

As described previously, in an attempt to derive a correlation for different types of specimens, critical strain approaches will often consider the data in terms of peak elastic stress, $K_t\sigma_{nom}$, allowing for a more direct correlation between plain specimen strain controlled data and material at the notch root. Figure 6 illustrates this type of approach for the current work and indicates a closer correlation between plain and notched specimen data, although the data still does not collapse completely. The clear difference in fatigue life between plain and VCN specimens in particular is an indicator that considering the peak elastic stress at the notch root, is not an accurate method of correlating notch specimen fatigue lives. This difference is often attributed to the volume of critically stressed material at the notch root. Fatigue is essentially probabilistic in nature and crack initiation usually occurs at a ‘weak link’, (microstructural, surface finish, defects etc) therefore statistically the smaller critically stressed volume of a VCN specimen is far less likely to contain a weak link than the

plain specimen which is critically stressed across the entire gauge length. The PD monitoring of specimens in the current work however allows for a more detailed investigation into these effects in the current material.

In order to derive a method for predicting fatigue life of notched components, it is clear that the stress control data generated is insufficient, and by the arguments discussed previously regarding the degree of constraint, attention should be turned to strain controlled fatigue of plain specimens. In the current programme only a limited number of strain controlled tests were able to be undertaken due to restrictions in the amount of material heat treated. However the results can be used as an indication of the predictive capability of this type of data with limited test numbers. Three tests produced valid data and an excellent fit to the data is given by the equation $\Delta\varepsilon = 0.0534N_f^{-0.187}$, with a correlation factor of $R^2=0.988$.

In predicting notched fatigue behaviour, the most popular traditional technique utilises the simplest form of the Manson-Coffin-Basquin [12-15] equation, as given in equation 1,

$$\Delta\varepsilon = C_pN_f^{\alpha1}+C_eN_f^{\alpha2} \quad (1)$$

where $\Delta\varepsilon$ is the total strain range, N_f is the number of fatigue cycles to failure and C_e, C_p, $\alpha1$, $\alpha2$ are fitting constants.

Strain control data can be partitioned into elastic and plastic components by analysis of stabilised stress-strain hysteresis loops in order to produce a relationship between strain range and fatigue life. However, this form of the equation is based on fully reversed loading, and calculations usually break down under the influence of significant mean stress, as would be the case in the current testing with R=0 loading preferred. Although adaptations such as the Morrow [16] form of the equation may be utilised, derivation of the equation is more difficult without R=-1 strain control data to accurately define the required constants. Therefore, for the current work, an alternative approach has been employed.

The Walker strain technique [17] has previously been shown to provide accurate predictions for non zero mean stress data [2, 3]. This approach has the advantage of primarily focussing on R=0 strain control fatigue data, with data from all other R ratios normalised to this condition. Clearly in the current work where the requirement is to predict the behaviour of R=0 notched specimens utilising R=0 strain control data, the possibility of using this technique is attractive.

The Walker strain relationship is an empirical method for correlating R values [18, 19]. The approach involves correlating strain control data of different R ratios using the expression

$$\Delta\varepsilon_w = \frac{\sigma_{\max}}{E}\left(\frac{\Delta\varepsilon E}{\sigma_{\max}}\right)^m \quad (2)$$

where:-
$\Delta\varepsilon_w$ = Walker strain
σ_{max} = maximum stabilised stress
E = Young's modulus
$\Delta\varepsilon$ = strain range
m = Walker exponent

The Walker exponent can be optimised by attempting to minimise the scatter in various R ratio data. However, with only a single set of R ratio data available this is clearly not possible in the current

work and it is necessary to consider values found within the open literature. Although no data is available for CSS42L, 300M is an alternative high strength steel which is comparable to CSS42L in terms of mechanical properties. Previous work [20] has shown that the Walker exponent (m) for this material is approximately 0.4, which falls within the range of usual values for the equation and is typical of a material which shows a dependence on both peak strain and strain range. As such, it seems reasonable to employ this value for predictions in CSS42L. Based on this m value, the predictive Walker strain equation takes the form

$$\Delta\varepsilon_W=0.0275N_f^{-0.146} \quad (3)$$

In the notched specimens utilised in the current work, it is critical that the stress-strain characteristics of the material at the notch root can be described accurately. Approximations can be made by one of the following two methods:-

i. For peak elastic stress values which do not exceed the yield stress, the apparent strain range of the material at the notch root can be calculated from $\Delta\varepsilon = \Delta\sigma/E$.
ii. For peak elastic stress values which exceed the yield stress, conditions at the notch root can be calculated either by FEA techniques, or more simply by analytical techniques which include applying Neuber's approximation [21] that the product of stress and strain at the notch root is a constant ($\sigma\varepsilon$=constant), or Glinka's [4-6] approach of constant strain energy.

Glinka's approach [4-6] has previously been shown to provide increased accuracy when providing input data for methods such as Manson-Coffin-Basquin [15] or Morrow [16]. However, in the current work, with the exponent for CSS42L estimated at 0.4, the Walker strain approach requires only definition of the peak stress, σ_{max}, for the fatigue cycle, provided elastic loading/unloading is then assumed for the remainder of the test. A combination of a low rate of strain hardening in the monotonic and cyclic stress-strain curves combined with minimal differences shown by the approaches of Glinka and Neuber leads to a strong similarity between the two approximations. Either approach could be utilised effectively, and as such both have been employed in the current work with the Glinka approach expected to provide more conservative predictions.

Predictions made for the fatigue lives of the notched specimens are shown in Table 4. Although the Walker strain approach appears to underpredict the fatigue lives of DEN and VCN geometries, it should be considered that predictions based primarily on strain control data will be accurate only for fatigue crack initiation in the notched testpieces. In a plain specimen, when a crack forms, it will advance though material which has also been critically stressed for the duration of the test and therefore the crack propagates quickly to failure. Conversely, in a notched specimen, the crack advances through material experiencing stresses considerably lower than that experienced at the notch root. Consequently a significant propagation phase should be considered for all notched geometries. It should also be considered that the ratio of initiation/propagation is likely to vary between different geometries since the stress gradient for each specimen along with the type of constraint (i.e. circular or rectilinear notch root section) will affect the crack propagation phase.

It is perhaps useful to consider that the use of K_t, the elastic stress concentration factor, may not be wholly adequate in the current set of predictions and that consideration should be made of the notched fatigue reduction factor, K_f. In the current specimens, this allows for the calculation of q, where

$$q=\frac{K_t-1}{K_f-1} \quad (4)$$

Table 5 indicates the calculated q values for the three notch geometries. Interestingly it can be seen that for the VCN notch, $q\approx1$ and so $K_f\approx K_t$. Whilst the value for the DEN specimens is slightly higher at 1.28, it is noticeable that a significant difference occurs with the RCN specimen, which has a value of

1.73. Clearly on the basis of these figures the RCN geometry would be expected to behave differently to the DEN and VCN specimens, with increased bulk plasticity more likely.

The results in Table 4 indicate that the addition of a propagation life to the predictions made for the VCN and DEN specimens should result in reasonable predictions. However, predictions made for the RCN notched specimens already exceed the fatigue lives of the tested specimens, prior to the addition of a crack propagation life. It is clear that the type of critical strain approach previously described may not be applicable for this specimen. Indeed, further consideration of the specimen geometry indicates that the assumptions previously made may not longer be applicable. When considering the RCN tests, reference to the monotonic curve for the material indicates that yield occurs at approximately 950-1000MPa. Therefore, for many of the RCN specimen tests, the shallow stress gradient in the specimen means that a significant volume of material is likely to experience bulk yielding, and therefore the conditions required to produce strain control deformation at the notch root are no longer achieved. This is also supported by the fact that the crack propagation phase of the tests on the RCN specimens are significantly shorter (approximately 27% of total life) than for example, the VCN specimen (approximately 46% of total life) indicating prior damage in the RCN specimen that accelerates the crack growth rate. Although the DEN specimen shows a reduced propagation life, this may be a factor of the square section geometry accelerating the rate of crack growth.

The potential difference plots, shown in Figure 5, therefore act as an excellent indication of the onset of long crack growth in the notched specimens. Considering that crack initiation seems to occur at approximately 54% of the total life in the VCN testpieces, 73% in the RCN and 92% in the DEN, propagation phases of 46%, 27% and 8% respectively should be added to the predictions shown in Table 4, providing separate predictions for each of the notch types, as given in Figure 7.

As discussed however, predictions made by the Walker strain approach are clearly not adequate for the RCN specimens. In this case improved predictions can be made by directly comparing the RCN specimen results with the load controlled fatigue data generated for plain specimens. Plotted on a stabilised stress range basis, Figure 6, it is clear that RCN geometries show a distinct similarity to the load control fatigue results. The RCN results do not compare directly to the strain control fatigue data, although this is most likely due to the fact that although the strain control tests are performed at an R ratio of zero (R_ε=0), since in plain specimens the resultant cyclic softening means that the stress R ratio becomes significantly more negative, and hence these tests show an extended fatigue life due to the reduction in mean stress. As described a crack propagation life of approximately 20% of total life should be added to the load controlled fatigue data, and the resultant predictions are still reasonable. The shorter lives shown in the RCN specimens may be related to a more complex stress state brought about by overall ratcheting of the specimen, or potentially a reduction in the quality of surface finish at the more difficult to polish notch root.

Clearly the notched specimen prediction falls into two separate categories. Provided the stress concentration is high enough, conditions akin to strain controlled deformation occur at the notch root and predictions made by methods such as the Walker strain technique provide a reasonable estimation of fatigue life. Interestingly, the traditional argument regarding the probability of a weak link being less in a smaller critically stressed volume, appears not to be the case here. Instead, the crack propagation phase in the VCN testpiece compared with the DEN (and certainly far more than a plain strain controlled specimen). Furthermore, this propagation phase constitutes 46% of the life in VCN specimens and therefore show the earliest onset of long crack growth of all of the specimens.

In notched testpieces where the stress concentration is lower (in the RCN, K_t=1.4) the degree of constraint necessary to produce strain controlled type behaviour does not occur due to a more

shallow stress gradient around the notch, and subsequent stress relaxation around the notch root. As such, direct comparison with plain specimen data appears to be the most effective approach. Correlation with R=0 strain control data does not provide adequate results since cyclic softening causes a negative stress R ratio to be applied for any specimens above yield in the plain specimen. Therefore, correlation with plain specimens loaded under load control at R=0 provides the most accurate results. In this case predictions of fatigue life are simply made based on a Basquin [14] type fit to the load control data.

Applying these two approaches to the data allows for an excellent comparison between the predicted notch specimen lives and those found from mechanical testing. Figure 8 illustrates the accuracy of the predictions with only the RCN specimens showing slightly longer fatigue lives than predicted. Although these predictions would normally be considered to be within the bounds of experimental scatter it is possible that the trend for slightly shorter lives than predicted in the RCN specimens is related to stress redistribution around the notch root which does not occur in plain test-pieces, or degraded surface finish.

5. Conclusions

The following conclusions can be drawn from the investigation:-

- Approaches to fatigue life prediction in CSS42L require consideration of both crack initiation and propagation phases. Previous techniques invoking arguments based on a smaller critically stressed volume in sharper notches, which is likely to contain less weak links, do not provide an adequate explanation.
- Prediction of the fatigue lives of notched specimens can be made by one of two techniques. For relatively low stress concentration features, direct comparison with stress control data at the same R ratio produces a reasonable estimation. In higher stress concentrations the Walker strain approach (or similar, depending on the input data) should be utilised to exploit the strain controlled conditions at the notch root.
- An exponent (m) of 0.4 in the Walker equation produces accurate predictions in the VCN and DEN specimens. This value appears consistent with a material that shows a significant dependence on mean stress, which is also evident from comparison of stress and strain controlled R=0 plain specimen data.
- Two techniques of predicting the stress-strain state at the root of notch were applied and gave similar results when applied using the Walker equation. The Glinka approach showed slightly more conservative predictions than the Neuber method.

6. References

[1] J-P Serey, Aerospace Engineering Article ‘Trends in Landing Gear Material’ September 2005.

[2] M.T. Whittaker, Considerations in fatigue lifing of stress concentrations in textured titanium 6-4, Int J Fatigue 33 (10) (2011) 1384-1391.

[3] M.T. Whittaker, P.J. Hurley, W.J. Evans, D. Flynn, Prediction of notched specimen behaviour at ambient and high temperatures in Ti6246, Int J Fatigue 29 (9-11) (2007) 1716-1725.

[4] G. Glinka, Energy density approach to calculation of inelastic strain stress near notches and cracks, Eng Fract Mech 22(3) (1985) 485-508.

[5] A. Newport, G. Glinka, Effect of Notch-strain Calculation Method on Fatigue-crack-initiation Life Predictions, Experimental Mechanics (1990) 208-216.

[6] G. Glinka, A. Newport, Effects of notch-tip stress-strain calculation method on the prediction of fatigue crack initiation life, Proceedings of 2nd International Conference on Low Cycle Fatigue and Elasto-Plastic Behaviour of Materials, Munich, Germany, September 1987.

[7] J.A.R. Duran, An energy-based approach for estimates of the stress-strain fields near crack-like notches, Mechanics of Solids in Brazil 2009.

[8] K. Golos, F. Ellyin, A total strain-energy density theory for cumulative fatigue damage, Trans ASME J Press Vess Tech 110(1) (1988) 36-41.

[9] M. Giglio, L. Vergani, Trans ASME Journal of Engineering Materials Technology 117 (1995) 50-55.

[10] J. Lemaitre, J-L. Chaboche, Mechanics of solid materials, UK: Cambridge Press; 1990.

[11] Z. Mroz, An attempt to describe the behaviour of metals under cyclic loads using a more general work hardening model, Acta Mech 7 (1969) 199-212.

[12] L.F. Coffin, Fatigue at High Temperatures, Fatigue at Elevated Temperature, ASTM STP 520 (1973) 5-34.

[13] S.S. Manson, Fatigue: A Complex Subject – Sample Simple Approximations, J. Exp. Mech. 5 (1965) 193-226.

[14] O.H. Basquin, The Exponential Law of Endurance Test, Proceedings of American society for testing and materials, Philadelphia, Vol. 10 (1919) 625-630.

[15] R. Basan, M. Franulovic, B. Krizan, On Estimation of Basquin-Coffin-Manson Fatigue Parameters of Low-Alloy Steel AISI4140, Proceedings of the 14th International Research/Expert Conference "Trends in the Development of Machinery and Associated Technology" TMT 2010, 11-18.

[16] J. Morrow, Fatigue properties of metals, section 3.2. In: Fatigue Design Handbook, Pub. No. AE-4. (1968) SAE, Warrendale,PA.

[17] K. Walker, The Effect of Stress Ratio During Crack Propagation and Fatigue for 2024-T3 and 7075-T6 Aluminium, Effects of Environment and Complex Load History on Fatigue Life, ASTM STP 462 (1970) 1-14.

[18] D.P. Shepherd, A. Wisbey, G.F. Harrison, T.J. Ward, B. Vermeulen, Cyclic Operation of Aero Gas Turbines – Materials and Component Life Implications, Mater High Temp, 18 (4) (2001) 231–239.

[19] P.J. Hurley, M.T. Whittaker, S.J. Williams, W.J. Evans, Prediction of fatigue initiation lives in notched Ti 6246 specimens, Int J Fatigue 30 (4) (2008) 623-634.

[20] N.E. Dowling, C.A. Calhoun, A. Arcari, Mean stress effects in stress-life fatigue and the Walker equation, Fatigue Fract Eng M 32 (3) (2009) 163-179.

[21] H. Neuber, Theory of Stress Concentration for Shear-Strained Prismatic Bodies with Arbitrary Nonlinear Stress-Strain Law, Transactions ASME, J. Appl. Mech. 28 (1961) 544-550.

Figure 1: Microstructure of tempered CSS42L

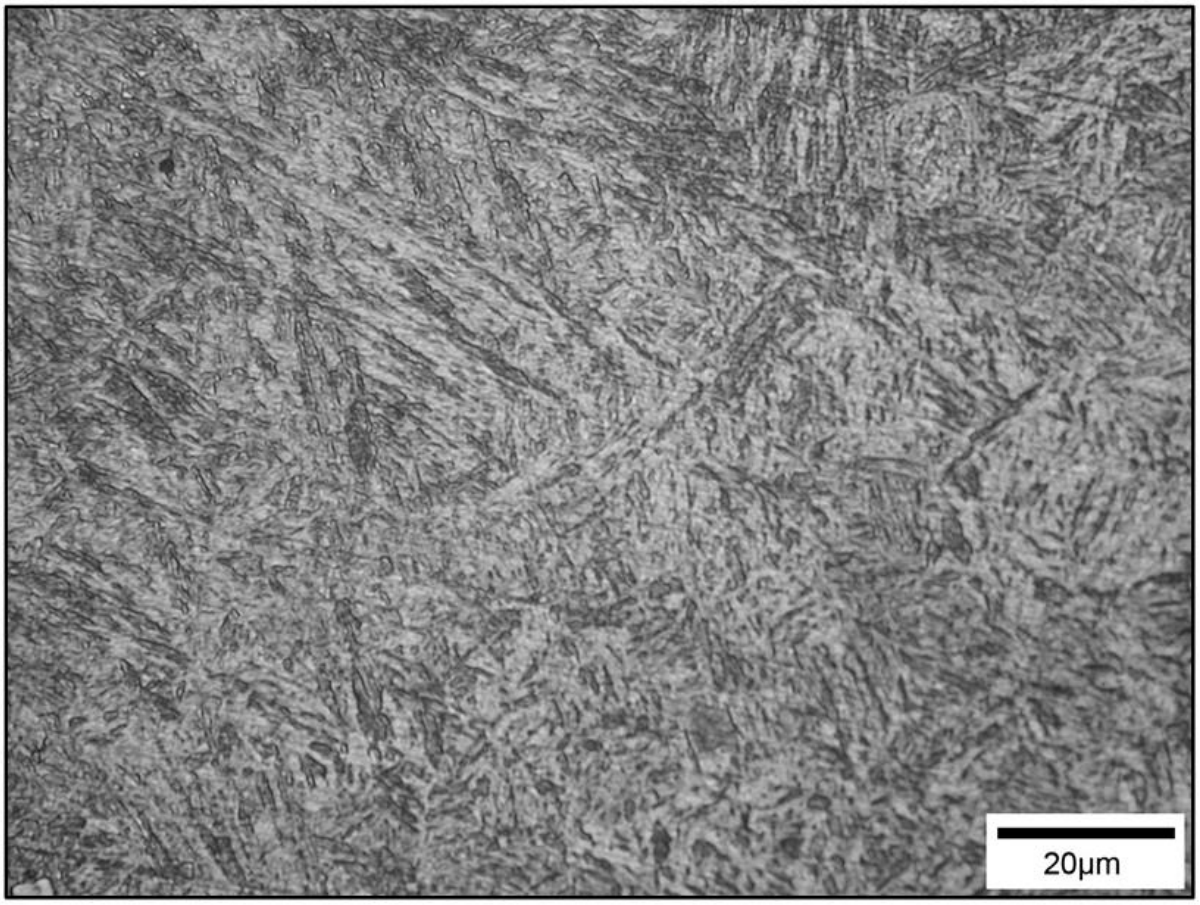

Figure 2: Specimen design for notched specimen testpieces (a) DEN, (b) RCN and (c) VCN

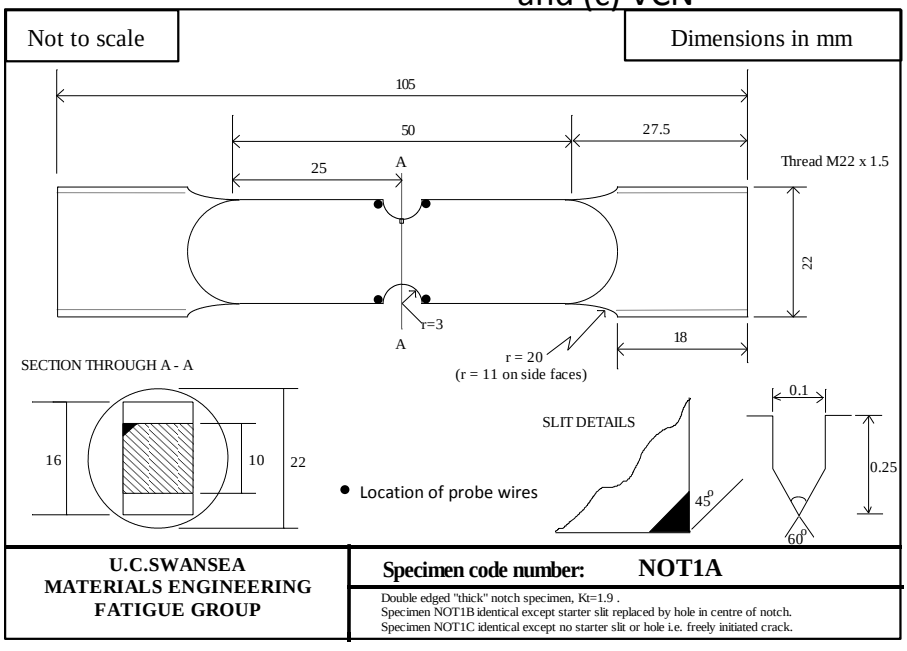

Not to scale

Dimensions in mm

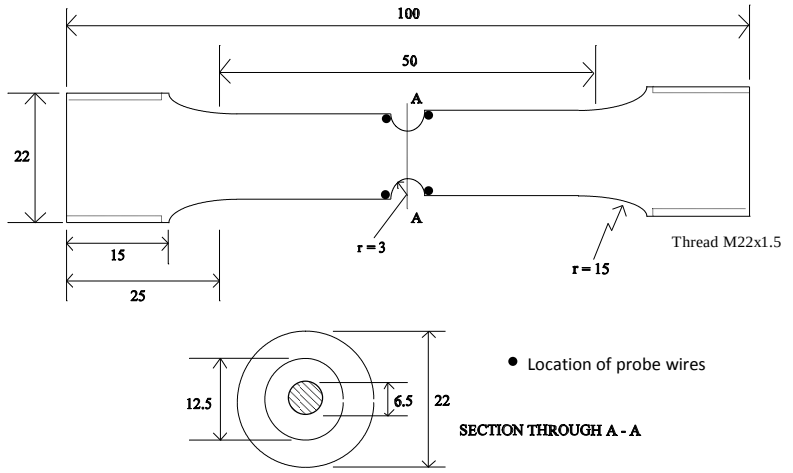

U.C.SWANSEA
MATERIALS ENGINEERING
FATIGUE GROUP

Specimen code number: NOT6

Semi-circular notch in round specimen, Kt=1.4
Circumference of notch root=total length of notch roots in NOT1.

Not to scale

Dimensions in mm

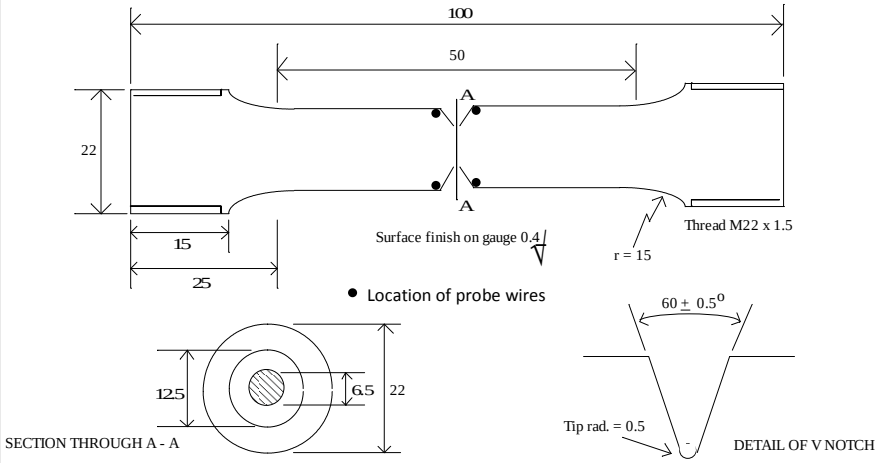

U.C.SWANSEA
MATERIALS ENGINEERING
FATIGUE GROUP

Specimen code number: NOT5

V notch in round specimen, Kt=2.7 .
Tip radius is critical, best machined by CNC profile cut not form tool, tolerance +/- 0.025mm.
Tolerances on all other dimensions +/- 0.1mm.

Figure 3: Hysteresis strain-stress loops for test 1

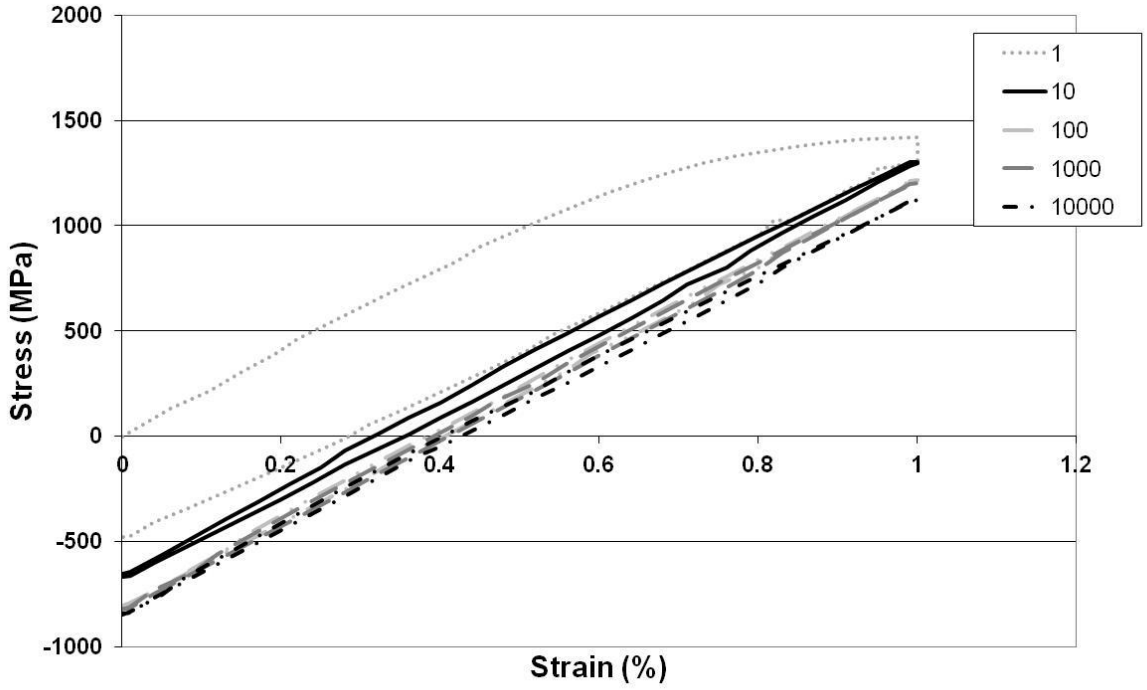

Figure 4: S-N fatigue response of plain LC, DEN LC, VCN LC, RCN LC and plain SC specimens, 20°C, R=0

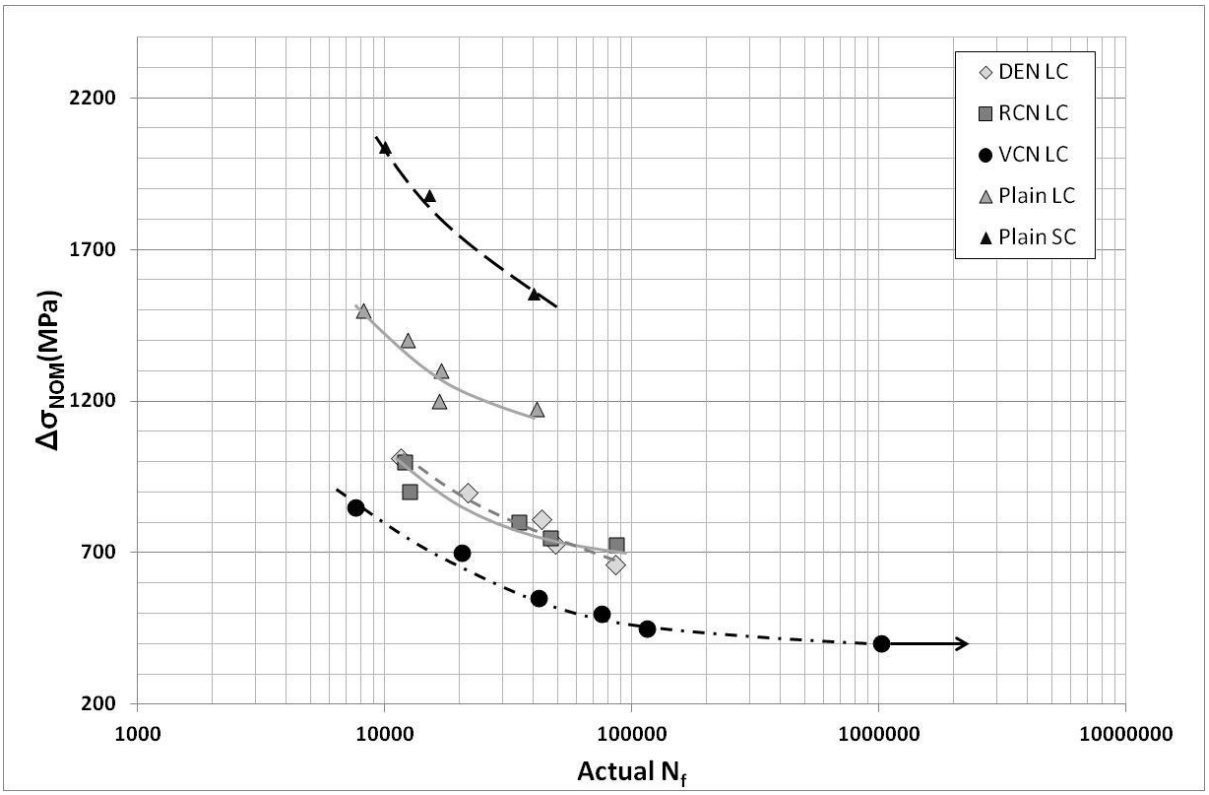

Figure 5: Potential difference as a function of number of fatigue cycles for (a) VCN, (b) RCN and (c) DEN specimens

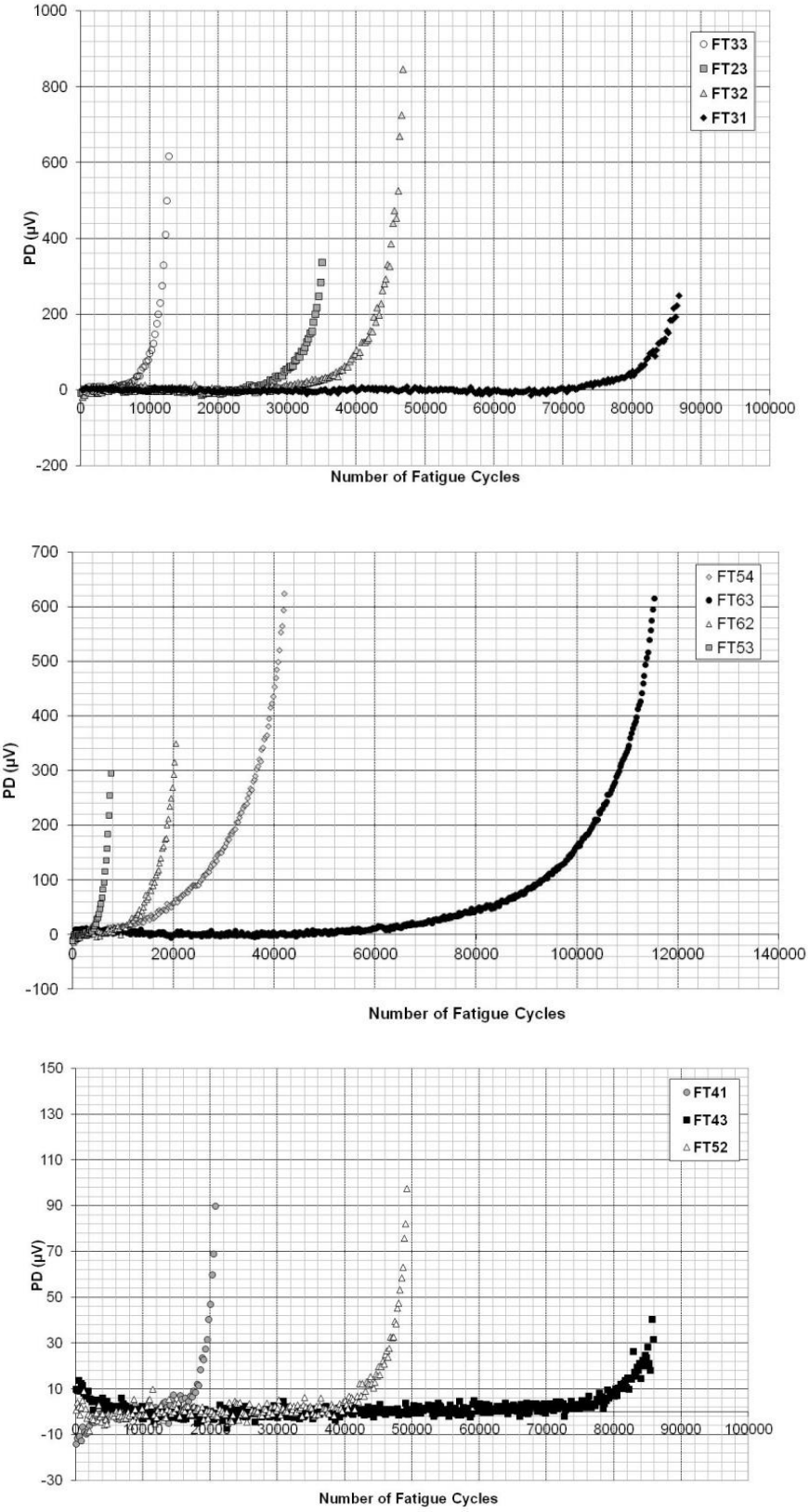

Figure 6: Peak elastic stress response of plain LC, DEN LC, VCN LC and RCN LC, 20°C, R=0

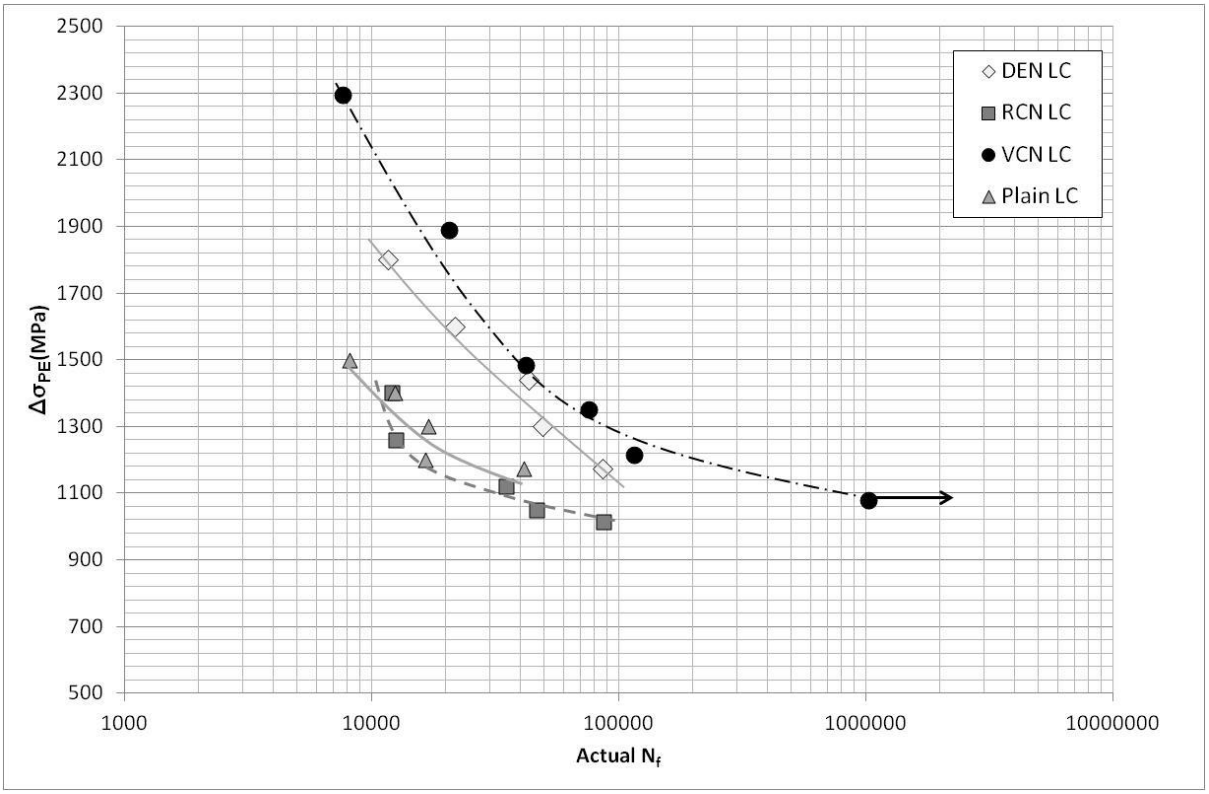

Figure 7: Predicted lives for DEN, RCN and VCN geometries with notch root conditions calculated by (a) Glinka approach (b) Neuber approach

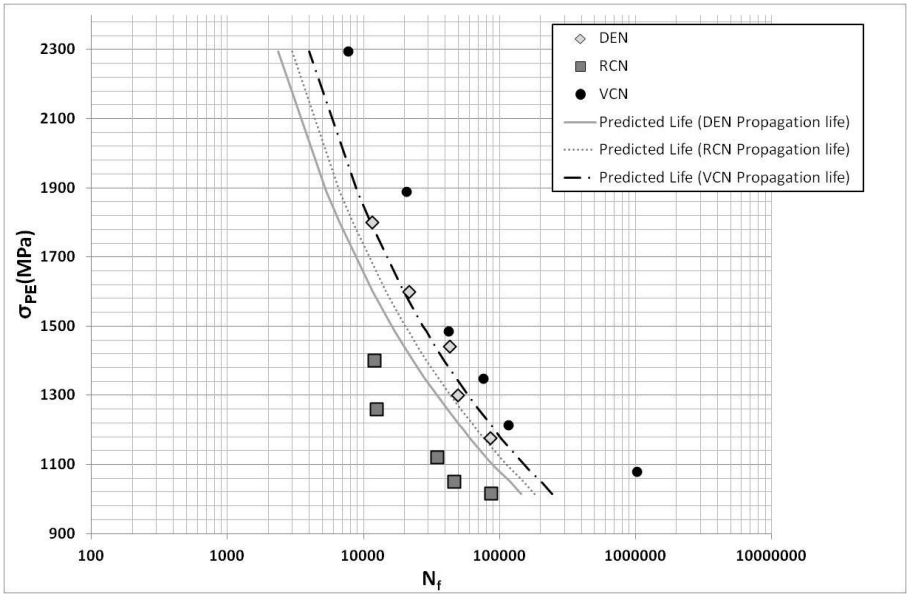

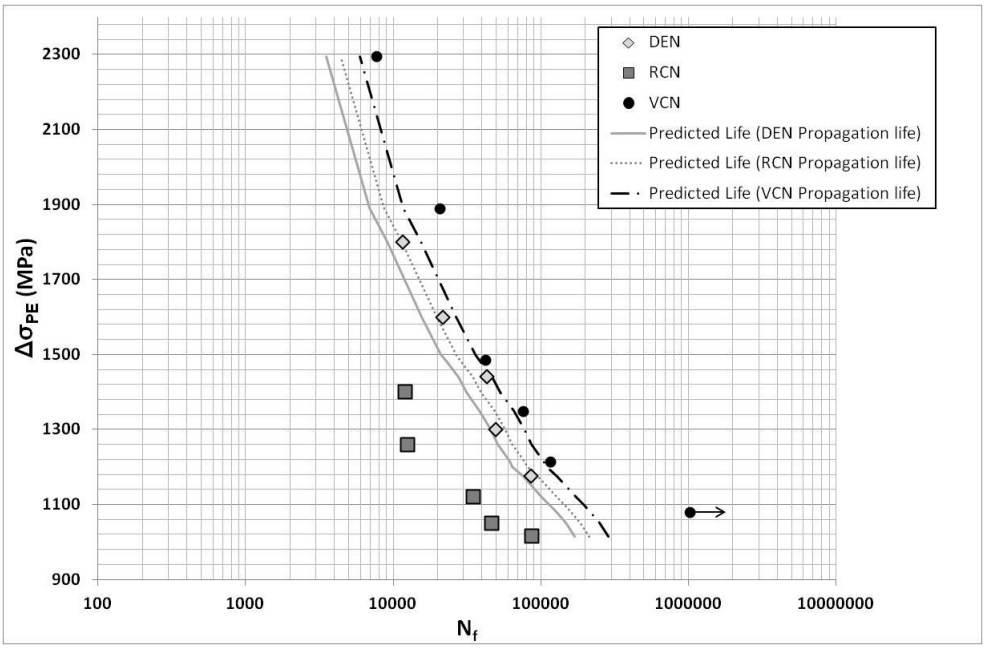

Figure 8: Final predicted lives for DEN, RCN and VCN notched specimens

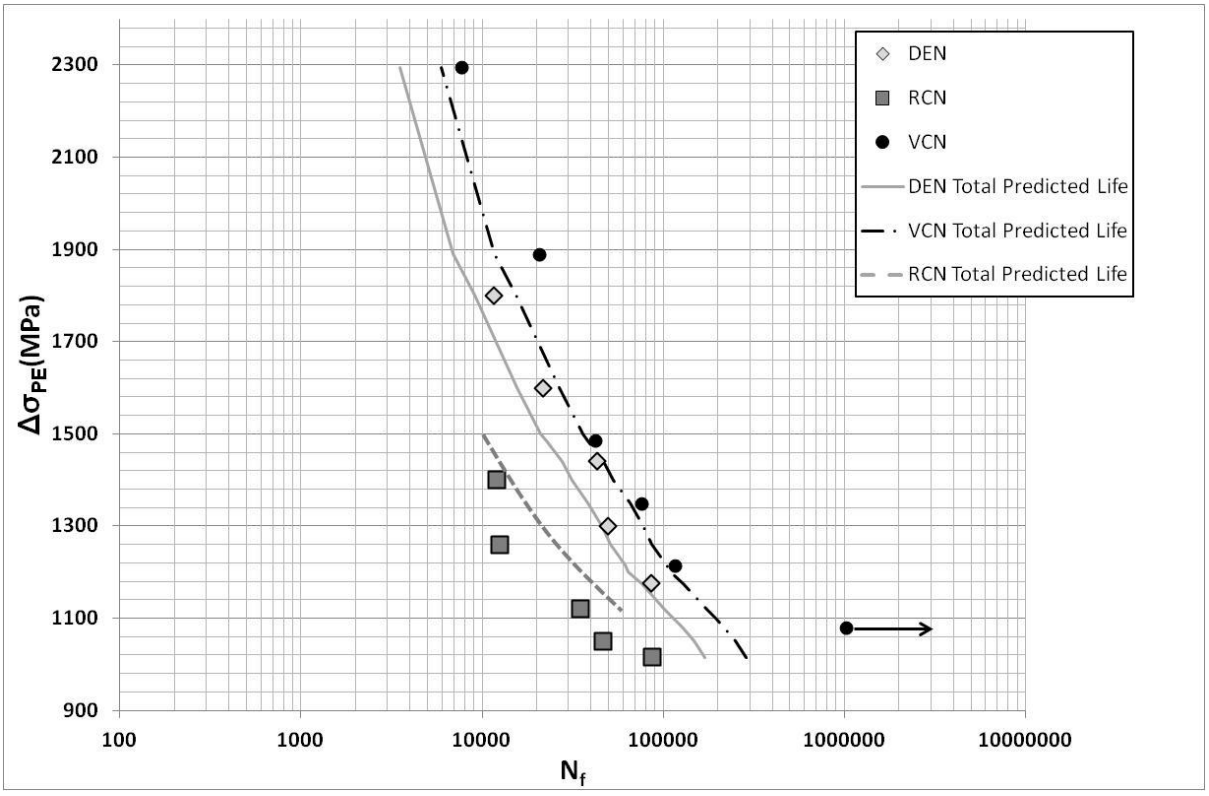

Table 1: Chemical composition of CSS42L

Ni	Cr	Mn	Cu	Mo	Nb	C	Si	P	S	Co	V	W	Fe
2.02	13.89	0.18	0.07	4.77	0.02	0.14	0.14	0.008	0.002	12.38	0.62	0.04	Bal

Table 2: Strain control results

Specimen ID	**R Ratio**	**ε_{MAX} (%)**	**$\sigma_{STAB\ MAX}$ (MPa)**	**$\sigma_{STAB\ MIN}$ (MPa)**	**$\Delta\sigma_{STAB}$ (MPa)**	**N_f**
1	0	1	1197	-840	2037	9989
2	0	0.65	1007	-546	1553	40231
3	0	0.75	1101	-776	1878	15200

Table 3: Initiation and propagation lives for DEN, RCN and VCN specimens

Specimen ID	**Type**	**Initiation (%)**	**Propagation (%)**	**Initiation (N)**	**Propagation (N)**	**N_f**
FT41	DEN	89	11	18500	2250	20750
FT52	DEN	91	9	45000	4200	49200
FT43	DEN	97	3	83000	2800	85800
Average		92				
FT23	RCN	80	20	28000	7000	35000
FT33	RCN	54	46	7000	5750	12750
FT31	RCN	86	14	74500	12250	86750
FT32	RCN	70	30	33000	13750	46750
Average		73				
FT54	VCN	40	60	16750	25250	42000
FT63	VCN	60	40	69250	46000	115250
FT62	VCN	56	44	11500	9000	20500
FT53	VCN	60	40	4600	3000	7600
Average		54				

Table 4: Walker Strain predictions for notched specimens

σ_{PE} (MPa)	Notch Geometry	Redistributed σ_{MAX} (MPa)	Walker Strain	Predicted Life (N_f)	Actual Life (N_f)
1015	RCN	925	0.0048	155742	86754
1050	RCN	935	0.0049	135793	46771
1080	VCN	952	0.0050	116734	1026656
1120	RCN	980	0.0052	93797	35051
1175	DEN	1020	0.0054	69783	85944
1215	VCN	1050	0.0056	56517	115295
1260	RCN	1072	0.0057	46979	12571
1300	DEN	1080	0.0058	41826	49249
1350	VCN	1097	0.0060	35372	75430
1400	RCN	1126	0.0061	28762	12083
1440	DEN	1139	0.0063	25399	43104
1485	VCN	1172	0.0064	20760	42031
1600	DEN	1220	0.0068	14350	21722
1800	DEN	1286	0.0074	8369	11634
1890	VCN	1332	0.0077	6337	20546
2295	VCN	1380	0.0085	3219	7647

Table 5: K_f and q values for DEN, RCN and VCN notch geometries

Geometry	K_f value	q value
RCN	1.69	1.73
VCN	2.75	1.03
DEN	2	1.28